MR No. E5L17

NATIONAL ADVISORY COMMITTEE FOR AERONAUTICS

WARTIME REPORT

ORIGINALLY ISSUED

February 1946 as
Memorandum Report E5L17

ALTITUDE-WIND-TUNNEL TESTS OF POWER-PLANT INSTALLATION IN JET-PROPELLED FIGHTER

By G. Merritt Preston, Fred O. Black, Jr.
and James M. Jagger

Aircraft Engine Research Laboratory
Cleveland, Ohio

NACA

WASHINGTON

NACA MR No. E5L17

NACA AIRCRAFT ENGINE RESEARCH LABORATORY

MEMORANDUM REPORT

for the

Air Technical Service Command, Army Air Forces

ALTITUDE-WIND-TUNNEL TESTS OF POWER-PLANT INSTALLATION IN JET-PROPELLED FIGHTER

By G. Merritt Preston, Fred O. Black, Jr.
and James M. Jagger

SUMMARY

Means for improving the power-plant installation in a fighter airplane have been investigated in the NACA Cleveland altitude wind tunnel. Revisions to the installation included: (1) a revised boundary-layer removal duct, which reduced the thickness of the fuselage boundary layer approximately 60 percent; (2) a redesigned nacelle inlet, which eliminated the high negative pressures that occurred on the lips of the original inlet and, when used in conjunction with the revised boundary-layer removal duct, increased the average pressure recovery at the compressor inlets approximately 16 percent; and (3) revised cooling-air seals, which reduced the amount of cooling air flowing through the nacelle approximately 75 percent without causing excessive nacelle temperatures. The replacement of one of the original nacelles by the revised nacelle reduced the uncorrected airplane drag coefficient approximately 0.0026 at a Mach number of 0.45.

INTRODUCTION

An investigation of the characteristics of a fighter airplane has been conducted by the NACA at the request of the Air Technical Service Command, Army Air Forces. The research program included clean-up tests (unpublished data) and stability and control tests (reference 1) made in the NACA Langley full-scale tunnel. An investigation of the aerodynamic characteristics of the power-plant installation in the Cleveland altitude wind tunnel is discussed in this report. The results are of general interest for installations that have double side fuselage inlets.

The original power-plant installation was tested and the results of these tests indicated several possible causes of unnecessary drag and low pressure recovery at the compressor inlets. The following revisions were therefore made and tested: (1) The fuselage boundary-layer removal duct was revised to reduce the internal duct losses; (2) the nacelle-inlet lips were redesigned to reduce the high negative pressure peaks that occurred over the original inlets; and (3) the engine cooling-air seal was revised to reduce the amount of cooling air flowing past the engine.

SYMBOLS

The following symbols are used in the investigation:

a_o	speed of sound in free-stream air, feet per second
C	wing root chord, 10.67 feet
C_D	drag coefficient, $\frac{D}{q_o S}$
ΔC_D	increment of drag coefficient
D	drag, pounds
F_c	compressibility factor
H	total pressure, pounds per square foot absolute
M_o	free-stream Mach number (V_o/a_o)
p	local static pressure, pounds per square foot absolute
p_o	free-stream static pressure, pounds per square foot absolute
Q_b	boundary-layer air flow, cubic feet per second
Q_c	cooling-air flow, cubic feet per second
q_c	free-stream impact pressure $\left(F_c \frac{1}{2}\rho_o V_o^2\right)$, pounds per square foot
q_o	free-stream dynamic pressure $\left(\frac{1}{2}\rho_o V_o^2\right)$, pounds per square foot
R_o	free-stream Reynolds number $\left(\frac{\rho_o V_o C}{\mu_o}\right)$

S wing area, 385 square feet

V_i velocity of air entering nacelles, feet per second

V_o free-stream velocity, feet per second

V_i/V_o nacelle-inlet velocity ratio

$\frac{H - p_o}{q_c}$ total-pressure coefficient

$\frac{p - p_o}{q_o}$ static-pressure coefficient

Q_b/V_o air-flow coefficient

α angle of attack of thrust axis relative to free-stream flow direction, degrees

μ absolute viscosity, pound-second per square foot

ρ mass density of air, slugs per cubic foot

CONFIGURATIONS AND INSTRUMENTATION

The YP-59A fighter airplane is powered by two jet-propulsion engines, each having a rating at sea level of 1650 pounds static thrust at an engine speed of 16,500 rpm and an air consumption of 34 pounds per second. The installation of the full-scale test airplane in the altitude wind tunnel is shown in figure 1 with the tail surfaces removed and the engine nacelles faired. Tests were conducted using the original configuration and a revised configuration, which includes: (1) a revised boundary-layer removal duct, (2) redesigned nacelle inlets, and (3) revised engine cooling-air seals.

Boundary-Layer Removal Duct

Preliminary tests indicated that the original boundary-layer removal duct (fig. 2 (a)) did not remove a sufficient quantity of the low energy air in the boundary layer because of high energy losses caused by approximately 270° of bends and flow restrictions in the duct. The revised boundary-layer removal duct (fig. 2 (b)) extends directly back from the inlet following the lower contour of the nacelle and discharges behind the engine baffle.

A jet augmenter included in the revised design (fig. 3) pumped air from the rear nacelle compartment into the tail pipe, thus acting as a pump for the revised boundary-layer removal duct.

Total-pressure rakes were installed at the entrance to the boundary-layer removal duct. These rakes were used in conjunction with the nacelle-inlet rakes to measure the thickness of the fuselage boundary layer. Instrumentation was provided at the duct exit to measure the quantity of air flowing through the duct.

Nacelle Inlets

A comparison of the original and revised nacelle inlets is presented in figure 4. Stations and ordinates of the revised lip contours for the sections shown in figure 4 are given in table I. In order to improve the flow characteristics of the nacelle inlets, the inlet velocity ratio was increased by reducing the area of the inlet from 2.7 square feet to 1.8 square feet; in order to improve the pressure recovery at high angles of attack, the plane of the inlet was tilted at an angle of 8.5° with respect to the thrust axis as compared with 5° for the original inlet.

Instrumentation was provided at the left nacelle inlet to measure the static-pressure and total-pressure distributions and the temperature of the entering air. Flush orifices were installed on the lips of the right nacelle inlet to measure the surface-pressure distribution at sections A to E (fig. 4).

Engine Cooling-Air Seals

A seal restricting the flow of cooling air for the tail pipe and the rear of the nacelle is located just behind the rear compressor inlet. The original seal extended only to the perimeter of the engine, thereby leaving an annulus between the engine and the nacelle through which an excessive amount of cooling air flowed. As a means of reducing this air flow and its consequent internal drag, the revised seal was extended to the inner surface of the nacelle and engine cooling was provided by air leaving the boundary-layer duct exit and two ducts of 5 square inches each placed in the seal at the top of the engine between combustion chambers 2 and 3 and 8 and 9. Instrumentation was provided in these ducts to measure the quantity of cooling air.

TESTS

Power-off tests were made with the engine nacelles faired to determine a reference drag value for drag measurements obtained for the two nacelle configurations.

Power-on tests were made for the original and revised configurations. The tests were made at pressure altitudes from 5000 to 30,000 feet, velocities from 100 to 390 miles per hour, engine speeds from 13,675 to 16,410 rpm, and angles of attack of 0°, 2°, and 8°.

Because the wind-tunnel refrigeration equipment was not completed when these tests were conducted, altitude temperatures could not be simulated.

RESULTS AND DISCUSSION

Internal Air Flow

The inlet velocity ratios of the original and revised nacelles at various free-stream velocities are shown in figure 5. The combined effect of the decrease in nacelle-inlet area and the decrease in the flow of engine cooling air with the revised configuration was to increase the nacelle-inlet velocity ratio at the high speed of the airplane (595 ft/sec) from 0.53 for the original configuration to 0.58 for the revised configuration. The inlet velocity ratio at the high-speed condition of the revised nacelle is close to the optimum value of inlet velocity ratio given in reference 2 as 0.60 for this type of inlet.

Typical total-pressure profiles at the inlet to the original nacelle are shown in figure 6 for various inlet velocity ratios, Mach numbers, and Reynolds numbers. It is apparent from these surveys that at the low inlet velocity ratios, the boundary-layer removal duct was not removing all of the fuselage boundary layer with the result that some low energy air entered the engine air inlet. Tuft surveys made at conditions corresponding to high-speed flight showed separation and reversal of flow in the boundary layer ahead of the inlet. Total-pressure profiles at the inlet to the revised nacelle (fig. 7) show that at inlet velocity ratios as low as 0.50 practically all of the boundary layer is removed by the boundary-layer removal duct.

The average total-pressure coefficients obtained for the original and revised engine air inlets are presented in figure 8 for various inlet velocity ratios. High losses were encountered at the inlet of the original nacelle for inlet velocity ratios below 0.60

(fig. 8(a)). Sufficient removal of the boundary layer at the inlet to the revised nacelle decreased the total-pressure losses to approximately 0.01 q_c over the entire range of inlet velocity ratios tested (fig. 8(b)).

The effect of inlet velocity ratio on the thickness of the boundary layer in the plane of the inlet may be seen in figure 9. Boundary-layer thickness is defined as the distance from the fuselage to a point at which the total pressure is equal to free-stream total pressure. The increase in boundary-layer thickness at inlet velocity ratios of less than 0.8 for the original configuration is attributed to separation of the flow ahead of the inlet. These curves show that the boundary-layer thickness has been reduced from approximately 8 inches for the original configuration to approximately 3 inches for the revised configuration at the high-speed condition of the airplane.

Total-pressure profiles at the exits of the original and revised boundary-layer removal ducts are shown in figure 10. The total pressure of the air leaving the original duct was appreciably less than that of the air leaving the revised duct.

A comparison of the efficiencies of the original and revised boundary-layer removal ducts is shown in figure 11, in which the total-pressure drop coefficient is plotted against air-flow coefficient. For a given total-pressure drop coefficient, the air-flow coefficient of the revised duct was approximately four times that of the original duct.

The variation of the static-pressure coefficient at the exit of the revised boundary-layer duct with nacelle-inlet velocity ratio is shown in figure 12. For inlet velocity ratios corresponding to high-speed flight, these curves show that the static pressure at the exit of the duct was approximately equal to free-stream static pressure.

The variation of cooling-air flow with inlet velocity ratio is shown in figure 13. The cooling-air flow with the original configuration increased very rapidly as inlet velocity ratios corresponding to high-speed flight were approached. The cooling-air flow was reduced to approximately one-fourth of the original quantity when the revised cooling-air seals were installed without causing excessive nacelle temperatures.

The average total-pressure coefficients at the front and rear inlets of the compressor are plotted against nacelle-inlet velocity ratio in figure 14. At the high-speed condition, the average total-pressure coefficient of the front and rear compressor inlets was approximately 16 percent higher for the revised configuration than for the original configuration.

Typical total-pressure distributions around the front and rear compressor inlets for the original and revised configurations are shown in figures 15 and 16, respectively. The pressure recovery at the inboard side of the engines is low because the eccentric location of the engines in the nacelles caused greater pressure losses in the path through which the air passed to reach the inboard side of the engine intakes.

External Air Flow

Surface-pressure distributions over the five sections of the original and revised nacelle inlets shown in figure 4 are presented in figure 17 for various inlet velocity ratios at angles of attack of 0° and 2°. These surface pressures, which extend to 9 percent of the length of the nacelle, have been corrected for wind-tunnel constriction effect.

The data in figures 17(a) and 17(b) show that high negative pressure peaks occurred on all sections of the original nacelle lips and that the adverse pressure gradients behind these peaks were very high in most cases. At the high-speed inlet velocity ratio (0.53) the maximum negative pressure coefficient is approximately -1.13 at an angle of attack of 0° and approximately -1.82 at 2°.

The modifications to the inlet eliminated the pressure peaks that occurred over the lips of the original inlet (figs. 17(c) and 17(d)). The maximum negative pressure coefficients measured over a range of inlet velocity ratios tested was -0.29 at an angle of attack of 0° and -0.22 at 2°. The large reduction in the negative pressures resulted from the improved contour of the revised nacelle-inlet lips.

Nacelle Drag

The drag of the airplane is considered the difference between the calculated net engine thrust and the resultant force on the airplane as measured by the wind-tunnel scales. The variation of drag coefficient with Reynolds number for several configurations is shown in figure 18. The drag coefficients are based on uncorrected wind-tunnel data. These data, cross-plotted in figure 19 for a Reynolds number of 10,000,000, show that removing the fairings from one of the original nacelles increased the drag coefficient 0.0052 at a Mach number of 0.45. When the original nacelle was replaced with the revised nacelle, the drag coefficient reduced 0.0026.

SUMMARY OF RESULTS

From altitude-wind-tunnel tests of the power-plant installation of the fighter airplane conducted to investigate the aerodynamics of the original configuration and a revised nacelle configuration, the following results were obtained:

1. The revised boundary-layer removal duct reduced the thickness of the fuselage boundary layer in the plane of the nacelle inlets approximately 60 percent at the high speed of the airplane.

2. Use of the revised nacelle inlet and boundary-layer removal duct increased the average total-pressure recovery at the compressor inlets approximately 16 percent over the pressure recovery with the original configuration.

3. The revisions to the nacelle inlets eliminated the high negative pressure peaks that occurred over the lips of the original inlets.

4. The revised cooling-air seal reduced the quantity of cooling air approximately 75 percent without causing excessive nacelle temperatures.

5. When one of the original nacelles was replaced with the revised nacelle, the uncorrected airplane drag coefficient reduced approximately 0.0026 at a Mach number of 0.45.

Aircraft Engine Research Laboratory,
National Advisory Committee for Aeronautics,
Cleveland, Ohio.

REFERENCES

1. Brewer, Gerald W.: Langley Full-Scale-Tunnel Stability and Control Tests of the Bell YP-59A Airplane. NACA MR No. L5A18, Army Air Forces, Jan. 18, 1945.

2. Smith, Norman F., and Baals, Donald D.: Wind-Tunnel Investigation of a High-Critical-Speed Fuselage Scoop Including the Effects of Boundary Layer. NACA ACR No. L5B01a, 1945.

E-274

TABLE I - REVISED NACELLE-INLET LIP ORDINATES

[X, inside ordinate; Y, outside ordinate]

Station (in. from leading edge)	Section A		Section B		Section C		Section D		Section E	
	X	Y	X	Y	X	Y	X	Y	X	Y
0	0	0	0	0	0	0	0	0	0	0
.10	-.62	.60	-.31	.45	-.27	.37	-.31	.39	-.60	.62
.20	-.91	.73	-.44	.68	-.37	.53	-.44	.58	----	.90
.30	----	.93	-.53	.85	-.44	.66	-.53	.73	----	1.10
.40	----	1.10	-.60	.99	-.49	.77	-.58	.84	----	1.29
.50	----	1.24	-.66	1.11	-.53	.88	-.63	.94	----	1.45
.62	----	1.40	-.72	1.25	-.56	.99	-.68	1.06	----	1.60
.75	----	1.54	-.78	1.38	-.59	1.09	-.72	1.16	----	1.75
.88	----	1.68	----	1.49	-.61	1.19	-.74	1.24	----	1.87
1.00	----	1.83	----	1.59	-.62	1.27	-.77	1.34	----	1.98
1.25	----	2.07	----	1.80	-.65	1.44	-.80	1.50	----	2.18
1.75	----	2.44	----	2.14	-.68	1.73	-.84	1.77	----	2.49
2.50	----	2.98	----	2.58	-.69	2.07	-.85	2.15	----	2.85
3.25	----	3.38	----	2.98	-.69	2.38	-.83	2.48	----	3.14
4.00	----	3.75	----	3.34	-.65	2.65	-.81	2.80	----	3.39
4.75	----	4.08	----	3.70	-.62	2.88	-.78	3.08	----	3.59
5.50	----	4.39	----	4.02	-.58	3.10	-.74	3.34	----	3.77
6.50	----	4.76	----	4.40	-.51	3.36	-.66	3.65	----	3.97
7.50	----	5.13	----	4.76	-.43	3.60	-.56	3.92	----	4.17
8.50	----	5.50	----	5.10	-.32	3.83	-.44	4.16	----	4.35
9.50	----	5.85	----	5.40	-.22	4.05	-.32	4.38	----	4.51
10.50	----	6.19	----	5.70	-.11	4.24	-.18	4.58	----	4.65
12	----	6.65	----	6.10	.07	4.53	.03	4.86	----	4.87
14	----	7.25	----	6.64	.32	4.87	.35	5.20	----	5.12
16	----	7.82	----	7.15	.60	5.19	.69	5.50	----	5.36
18	----	8.35	----	7.63	.87	5.44	1.06	5.80	----	5.57
20	----	8.85	----	8.08	1.17	5.68	1.42	6.06	----	5.75
22	----	9.33	----	8.52	1.45	5.88	1.80	6.30	----	5.91
24	----	9.78	----	8.95	1.55	6.07	2.19	6.53	----	----
26	----	----	----	9.36	2.05	6.27	2.59	6.76	----	----
28	----	----	----	9.77	2.35	6.44	2.98	6.97	----	----
30	----	----	----	10.18	2.66	6.69	3.39	7.16	----	----
32	----	----	----	10.59	2.96	6.75	3.81	7.35	----	----
34	----	----	----	10.98	3.29	7.91	4.22	7.51	----	----
36	----	----	----	11.36	3.62	8.05	4.65	7.68	----	----

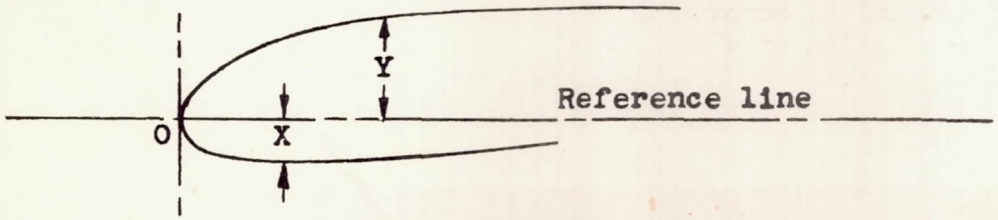

Reference lines parallel to thrust axis

NATIONAL ADVISORY
COMMITTEE FOR AERONAUTICS

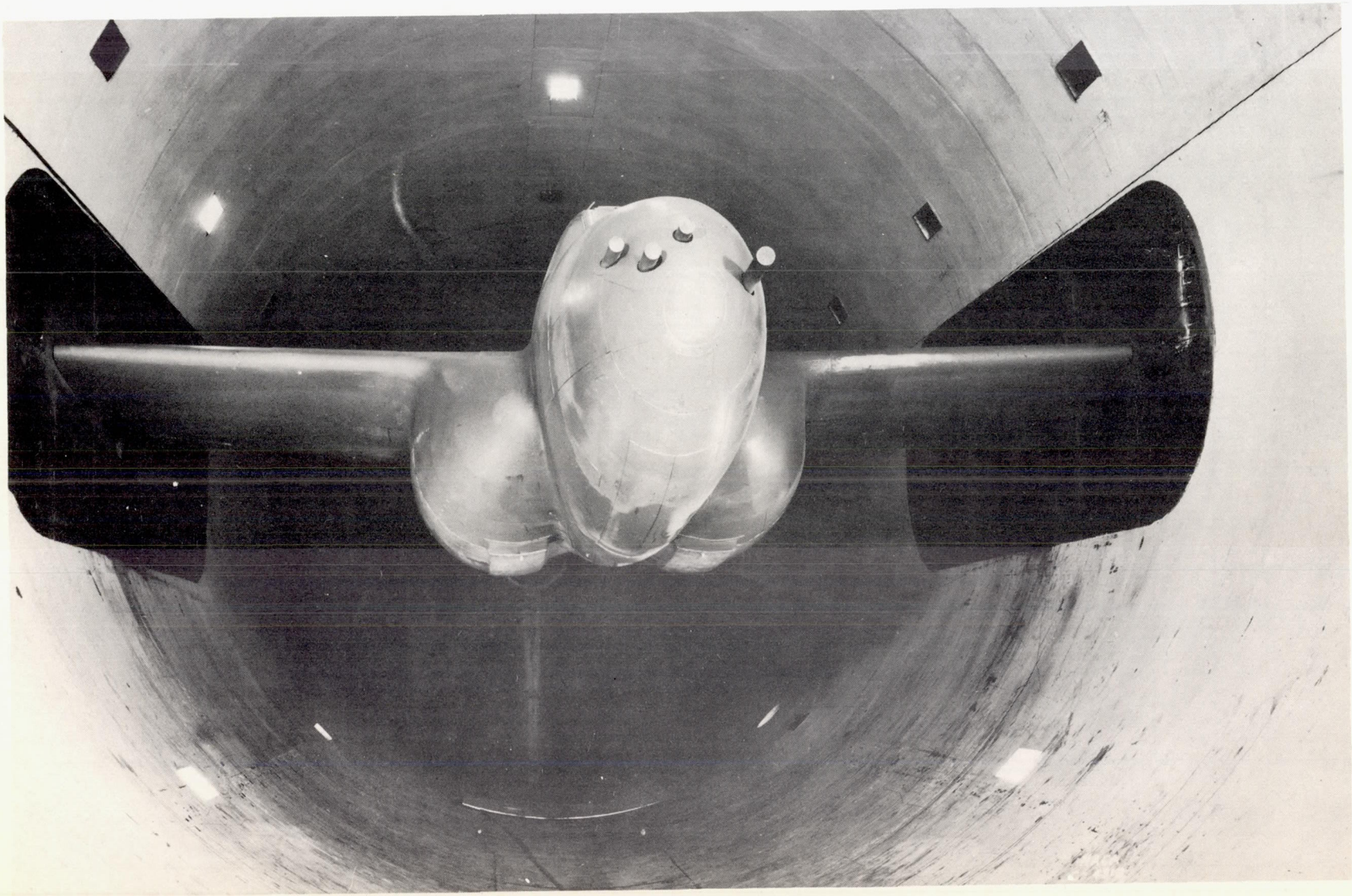

Figure 1. – Front view of fighter airplane with engine nacelles enclosed in fairings and mounted in altitude wind tunnel.

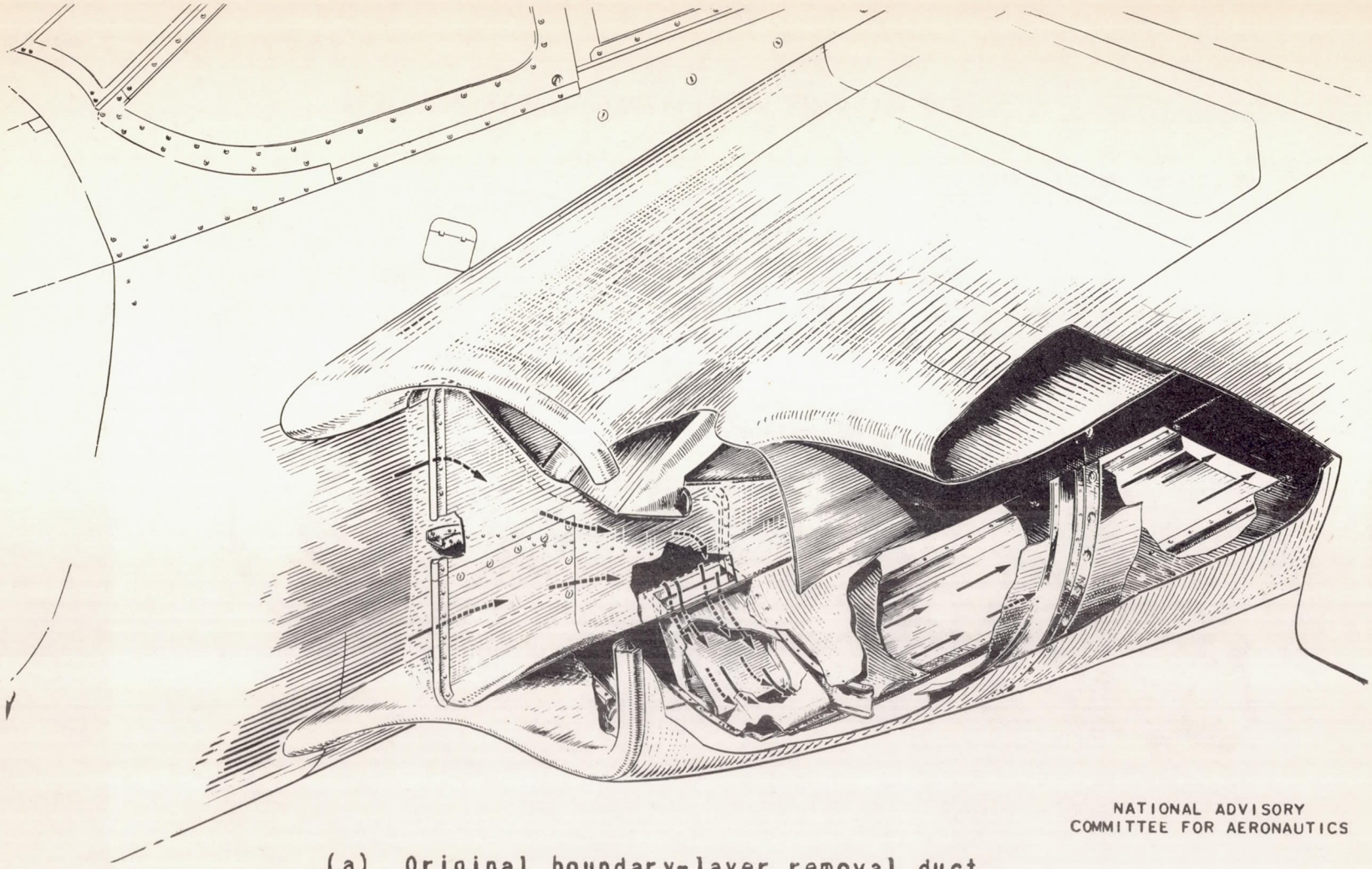

(a) Original boundary-layer removal duct.

Figure 2. - Cutaway view of boundary-layer removal duct and nacelle inlet of fighter airplane showing air-flow path through boundary-layer removal duct.

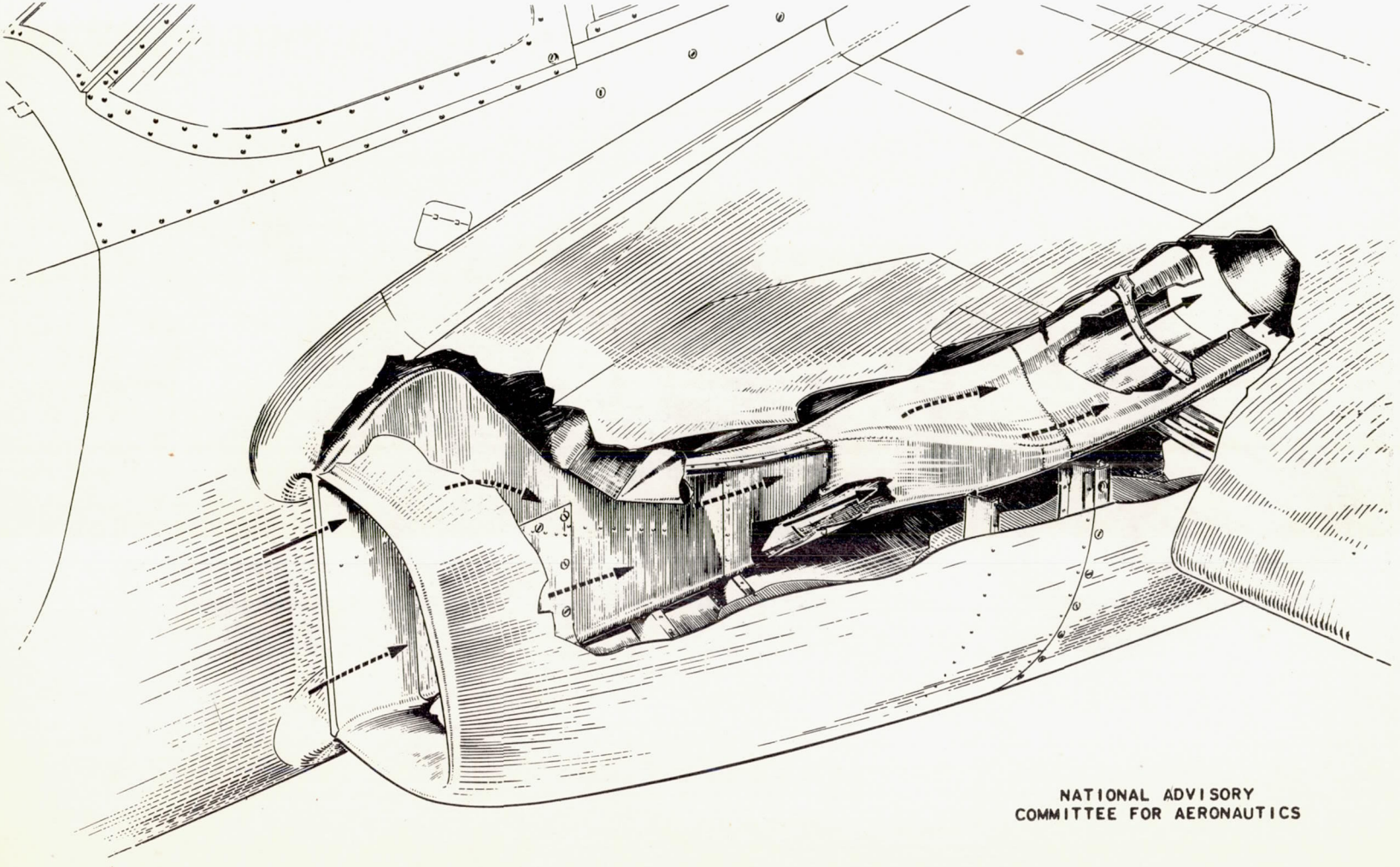

(b) Revised boundary-layer removal duct.

Figure 2. - Concluded.

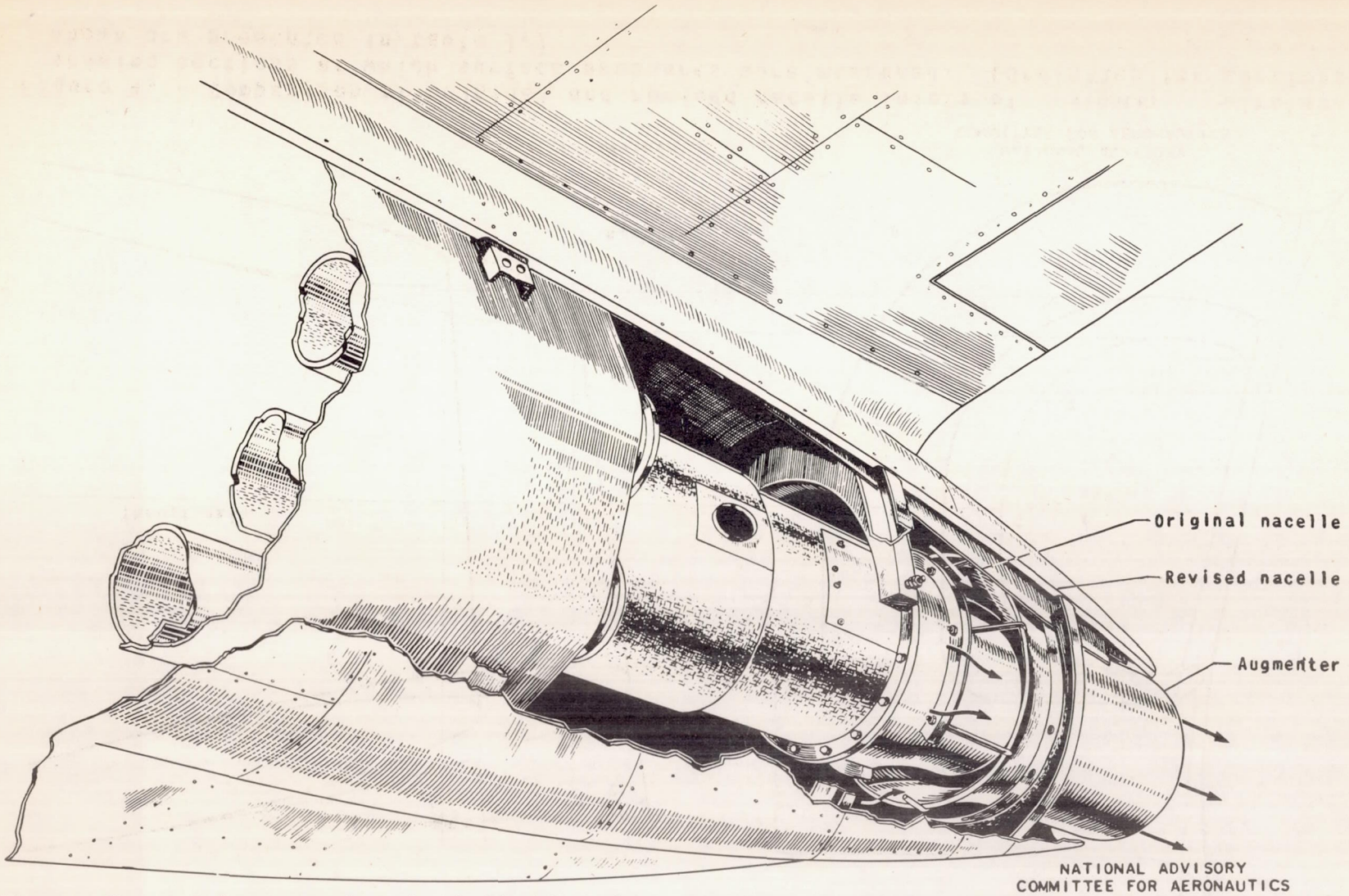

Figure 3. - Jet-augmenter installation in fighter airplane showing direction of air flow through augmenter.

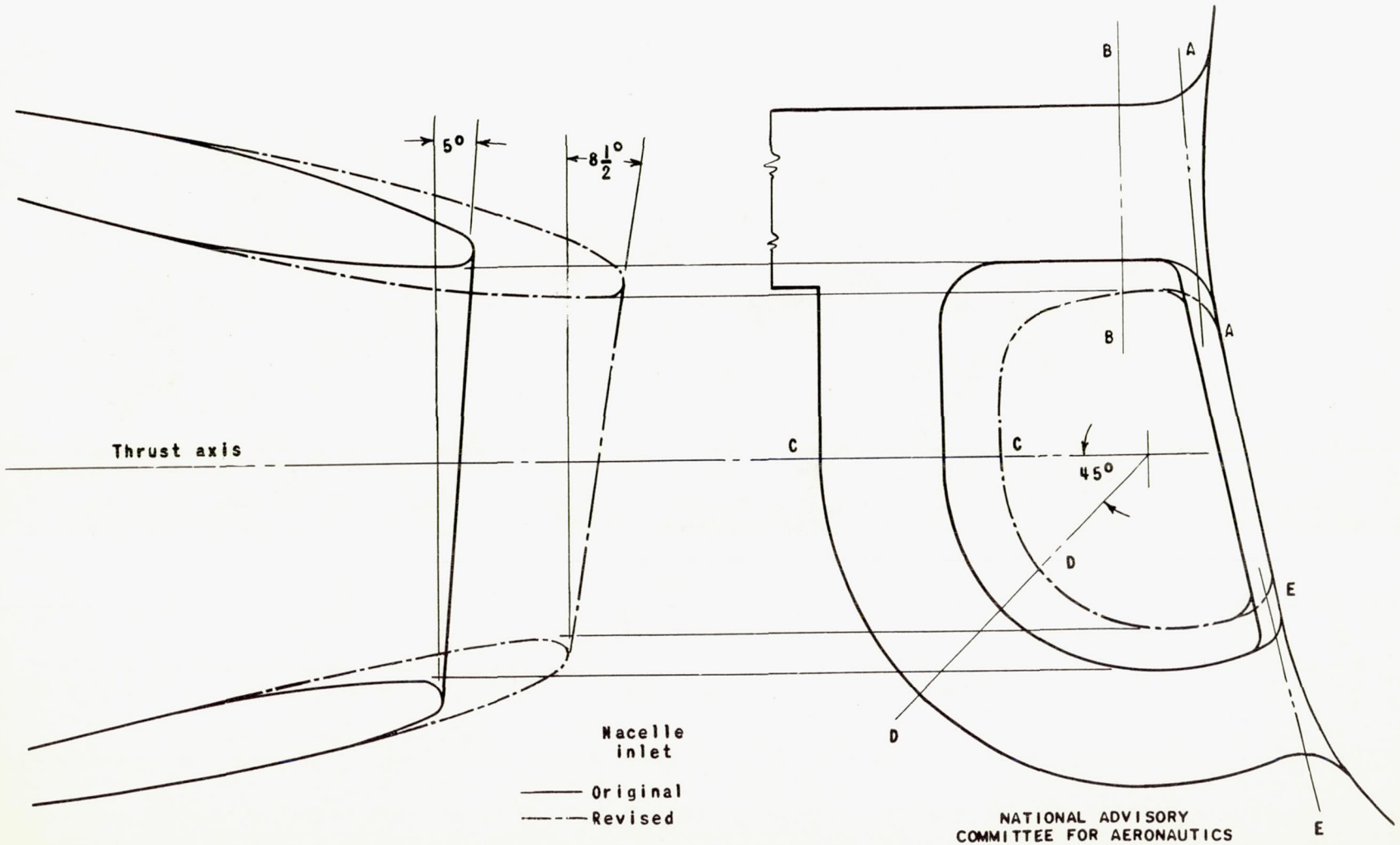

Figure 4. - Comparison of original and revised nacelle inlets of fighter airplane showing sections at which surface pressures were measured. (Ordinates for sections shown are presented in table I.)

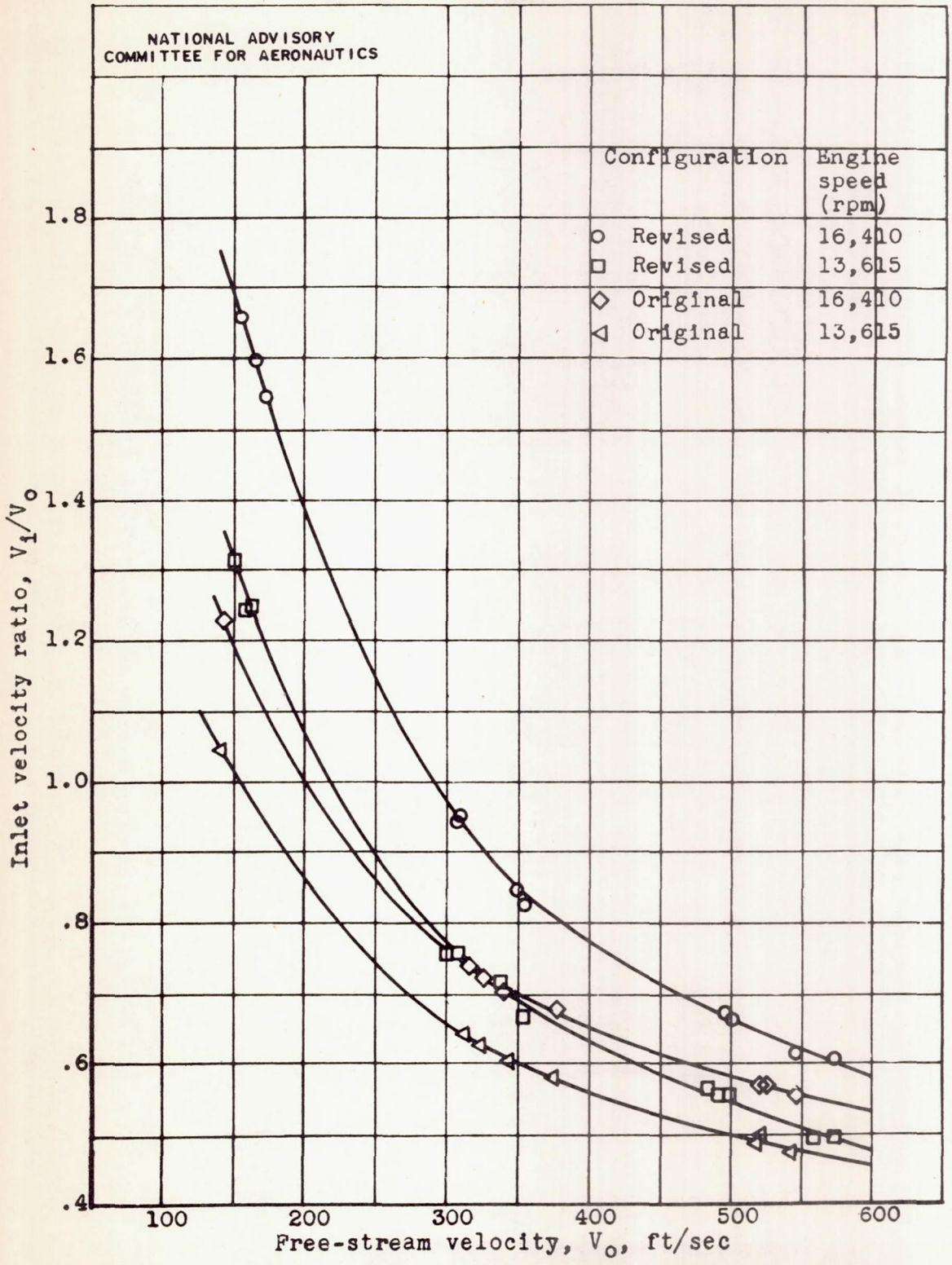

Figure 5.- Variation of nacelle-inlet velocity ratio with free-stream velocity of fighter airplane at angle of attack of 2°.

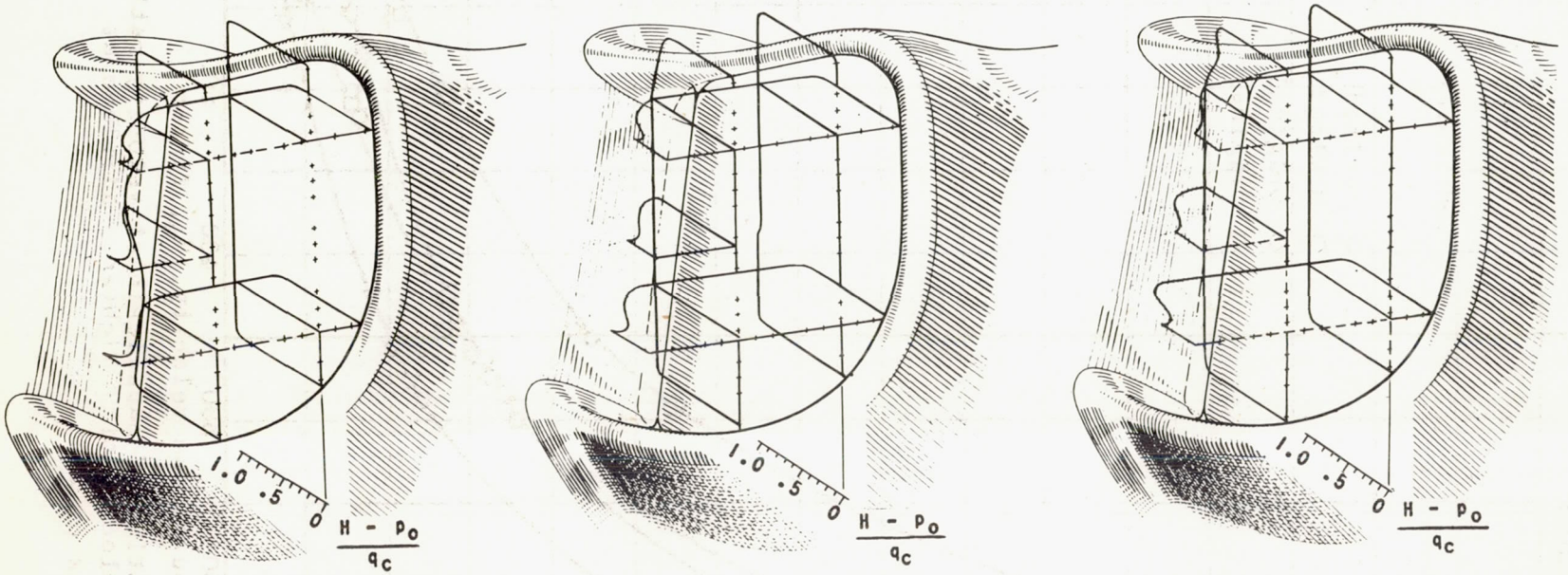

(a) Inlet velocity ratio, 0.45; Mach number, 0.46; Reynolds number, 8.6×10^6.

(b) Inlet velocity ratio, 0.54; Mach number, 0.42; Reynolds number, 13.7×10^6.

(c) Inlet velocity ratio, 0.74; Mach number, 0.27; Reynolds number, 14.5×10^6.

NATIONAL ADVISORY
COMMITTEE FOR AERONAUTICS

Figure 6. - Total-pressure distribution at original nacelle inlet of fighter airplane at angle of attack of 2°.

NACA MR No. E5L17

E-274

231+494

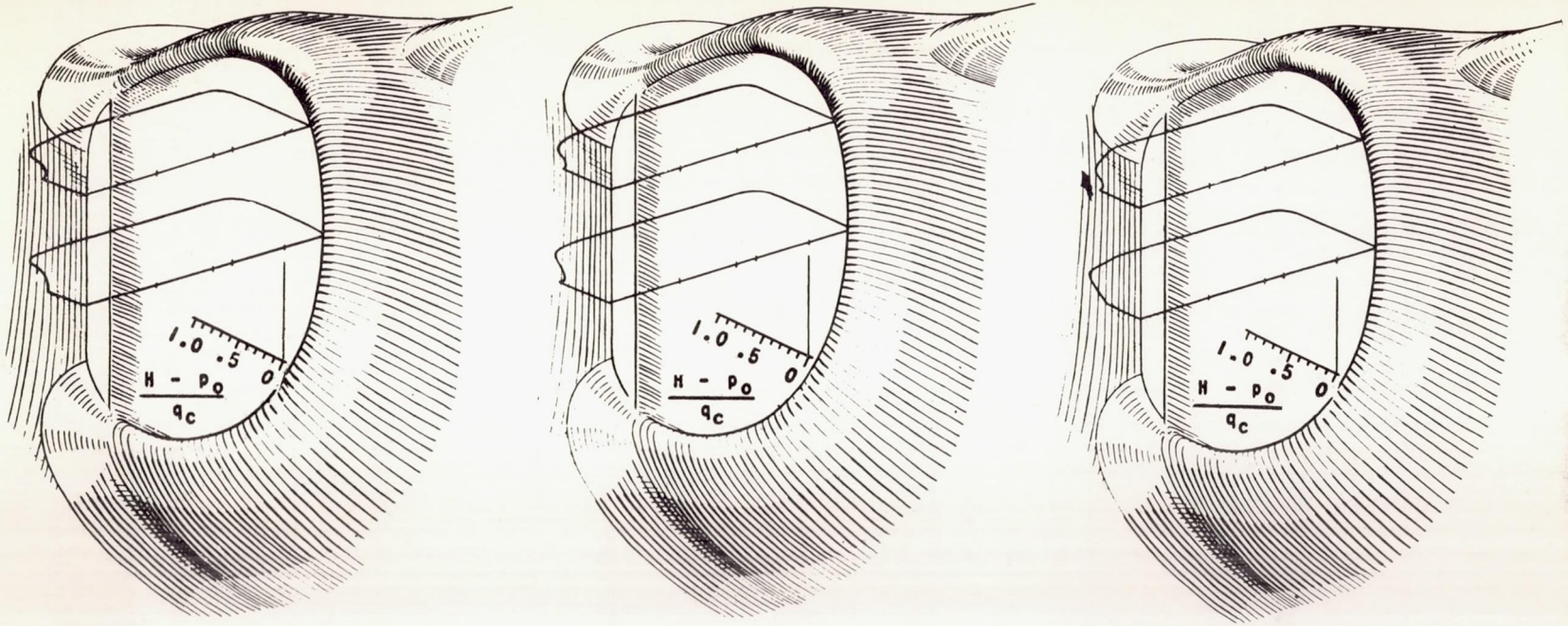

(a) Inlet velocity ratio, 0.50; Mach number, 0.49; Reynolds number, 9.5×10^6.

(b) Inlet velocity ratio, 0.65; Mach number, 0.42; Reynolds number, 15.3×10^6

(c) Inlet velocity ratio, 0.80; Mach number, 0.30; Reynolds number, 6.1×10^6.

NATIONAL ADVISORY COMMITTEE FOR AERONAUTICS

Figure 7. - Total-pressure distribution at revised nacelle inlet of fighter airplane at angle of attack of 2°.

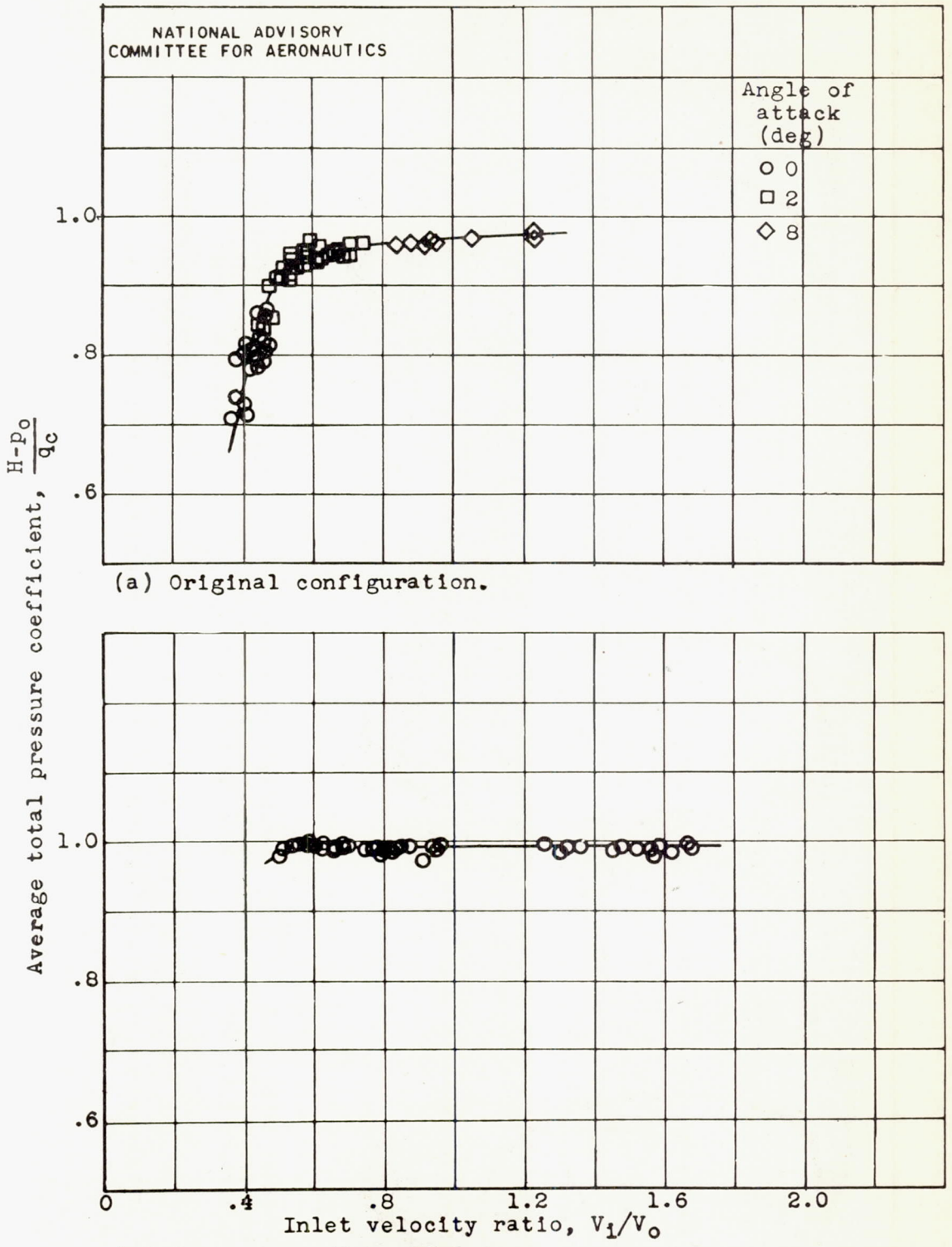

(a) Original configuration.

(b) Revised configuration.

Figure 8.- Variation of average total-pressure coefficient at nacelle inlet with nacelle-inlet velocity ratio of fighter airplane.

E-274

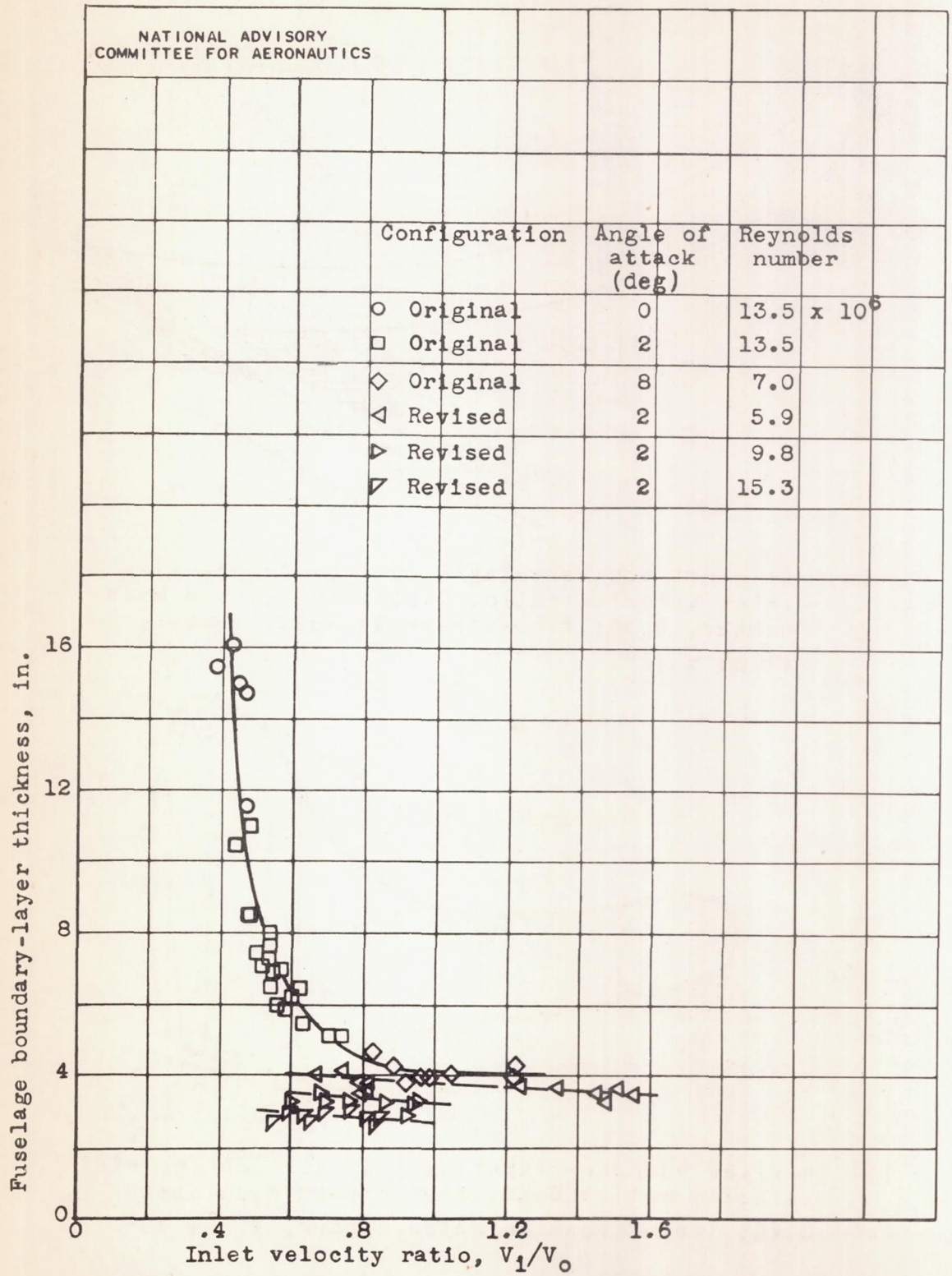

Figure 9.- Variation of fuselage boundary-layer thickness with nacelle-inlet velocity ratio of fighter airplane.

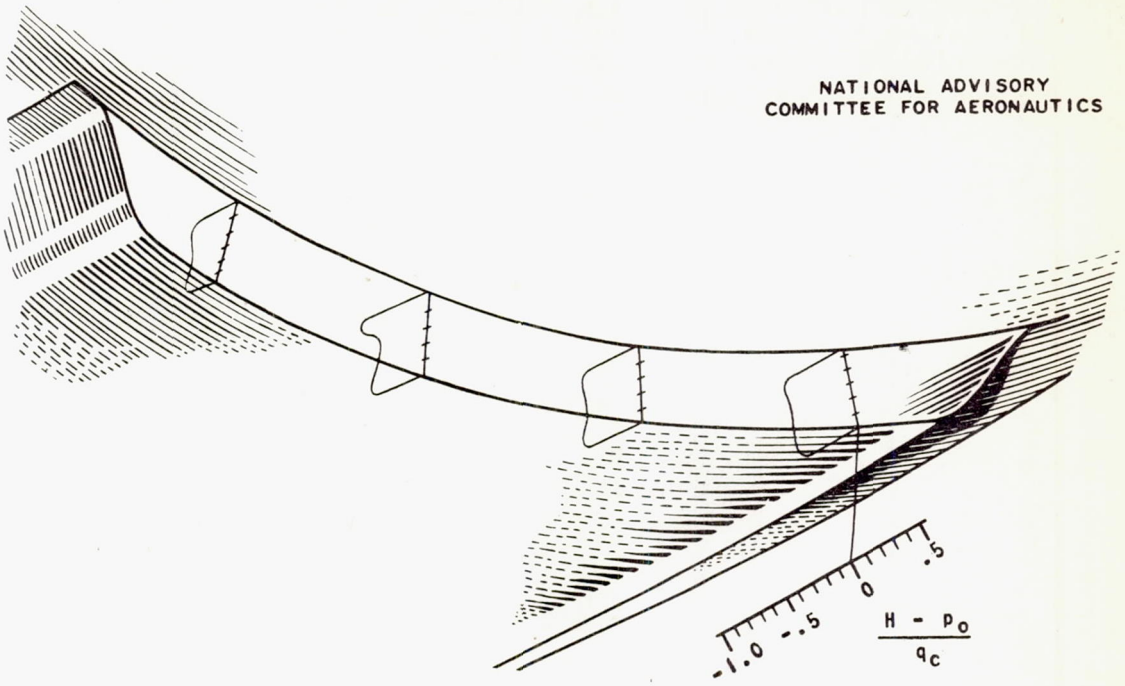

(a) Original boundary-layer duct exit; nacelle-inlet velocity ratio, 0.53; free-stream Mach number, 0.30; free-stream Reynolds number, 11.25×10^6.

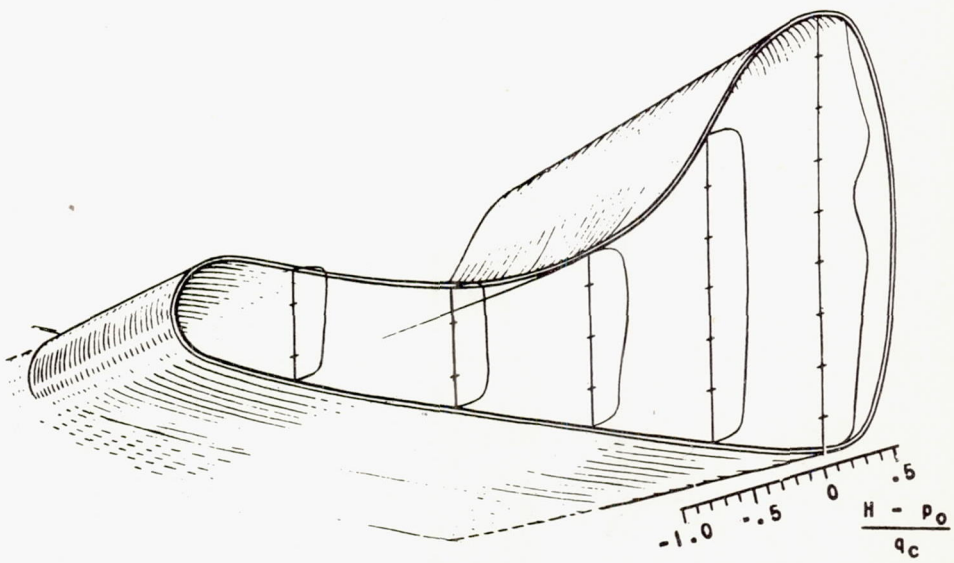

(b) Revised boundary-layer duct exit; nacelle-inlet velocity ratio, 0.50; free-stream Mach number, 0.49; free-stream Reynolds number, 9.5×10^6.

Figure 10. - Total-pressure distribution at exits of original and revised boundary-layer ducts of fighter airplane at angle of attack of 2°.

E-274

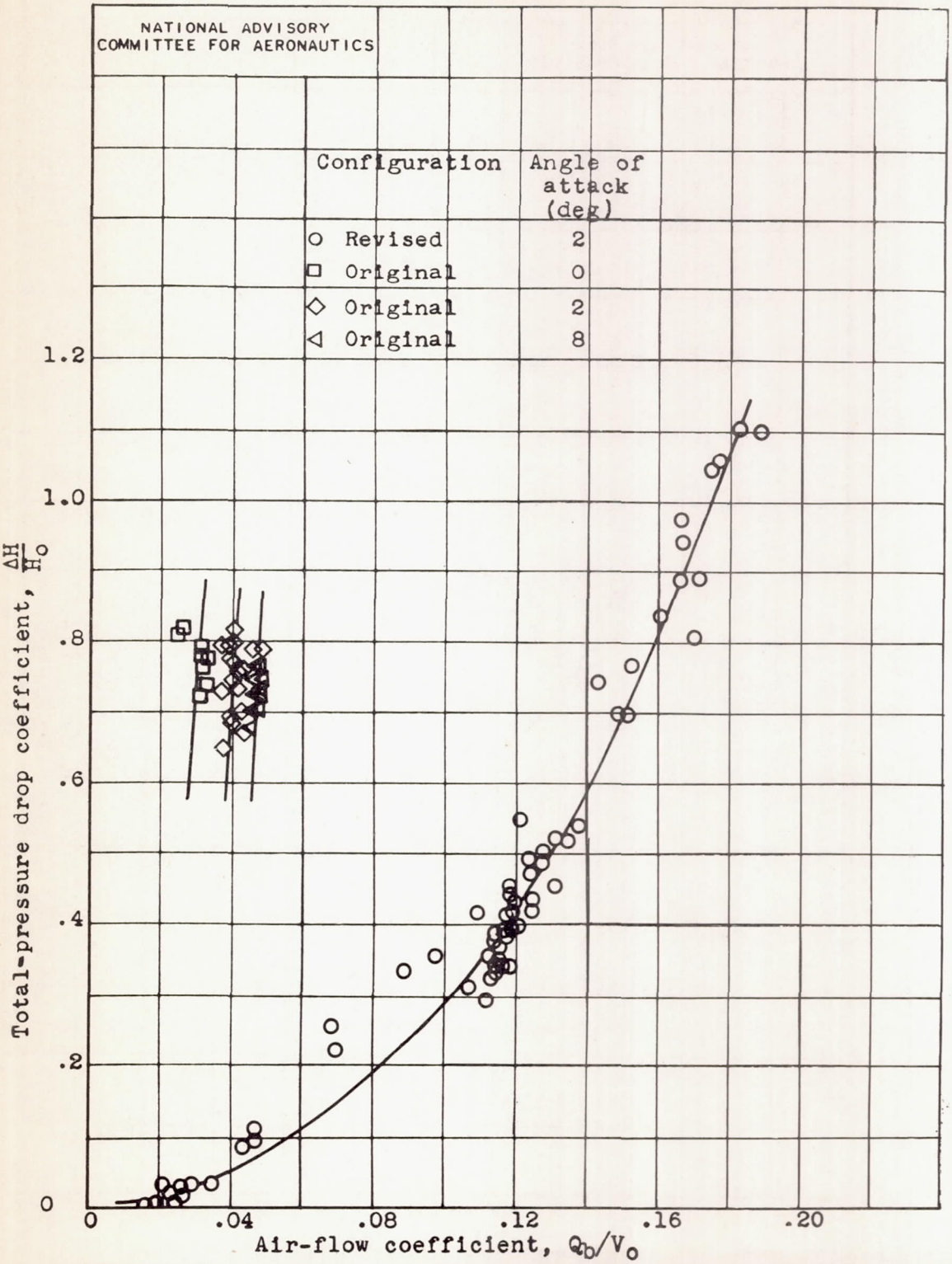

Figure 11.- Variation of total-pressure drop coefficient with air-flow coefficient for nacelle-inlet boundary-layer removal ducts of fighter airplane.

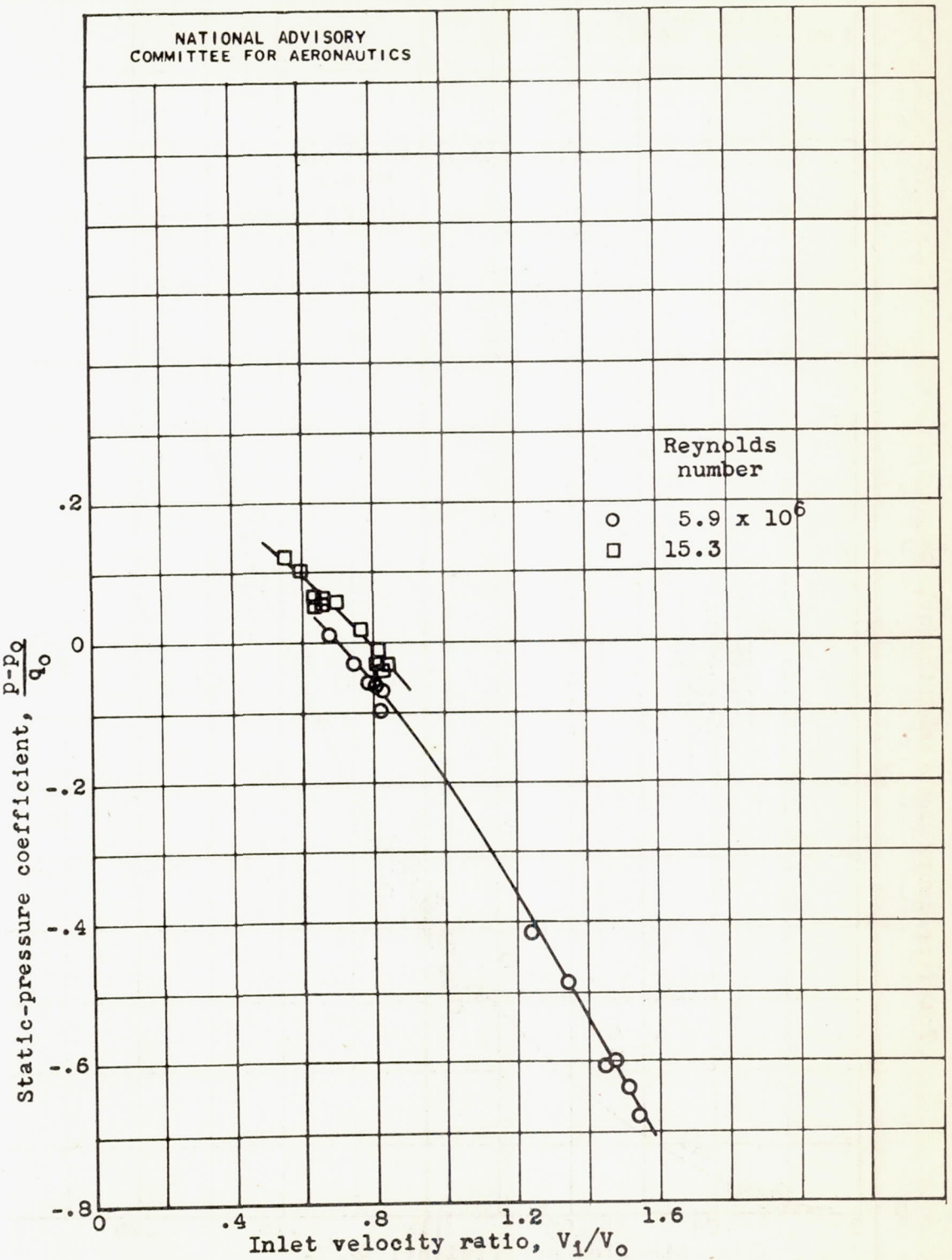

Figure 12.- Variation of static-pressure coefficient with nacelle-inlet velocity ratio at exit of revised boundary-layer removal duct of fighter airplane.

E-274

E-274

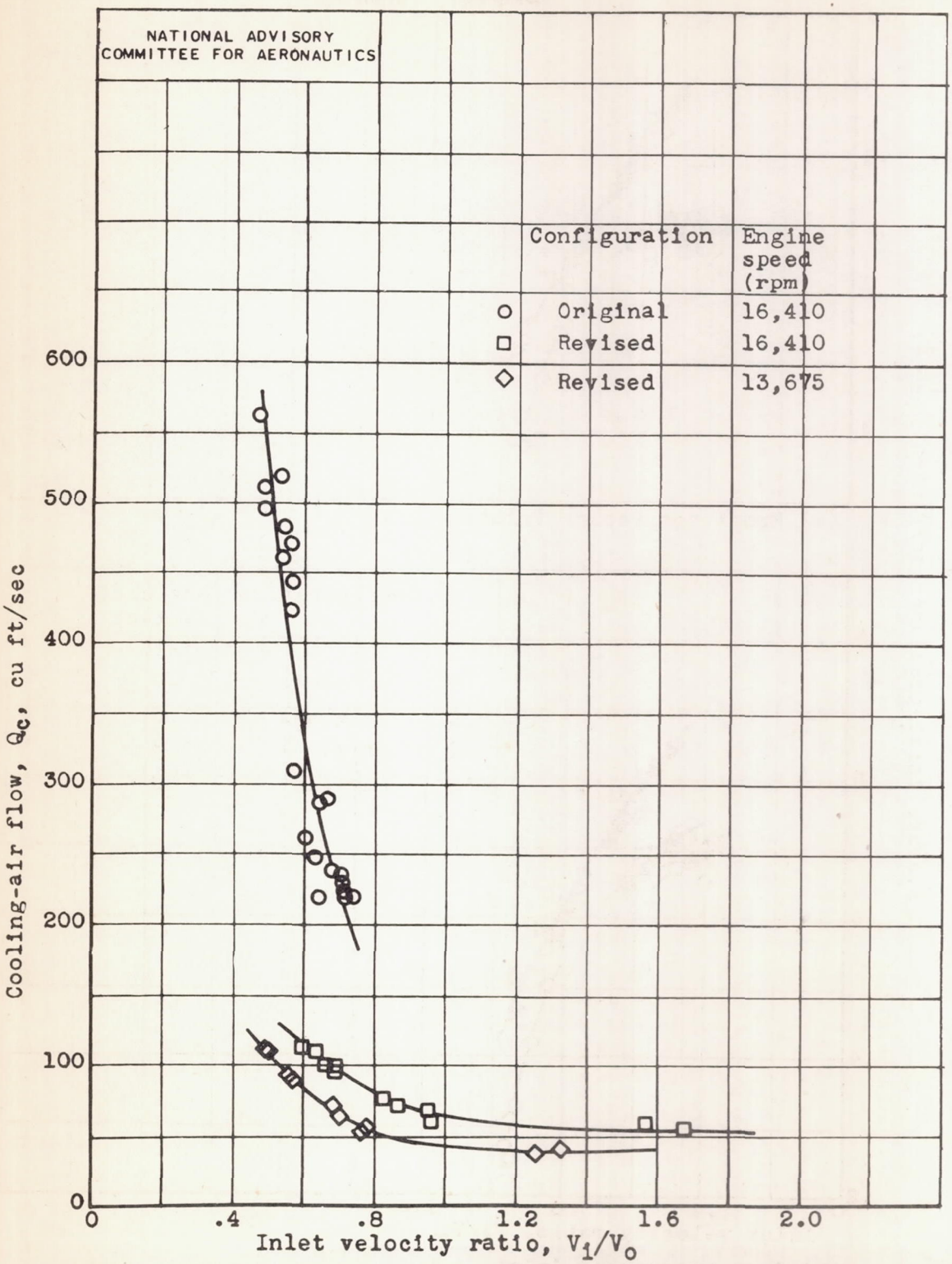

Figure 13.- Variation of cooling-air flow with nacelle-inlet velocity ratio of fighter airplane.

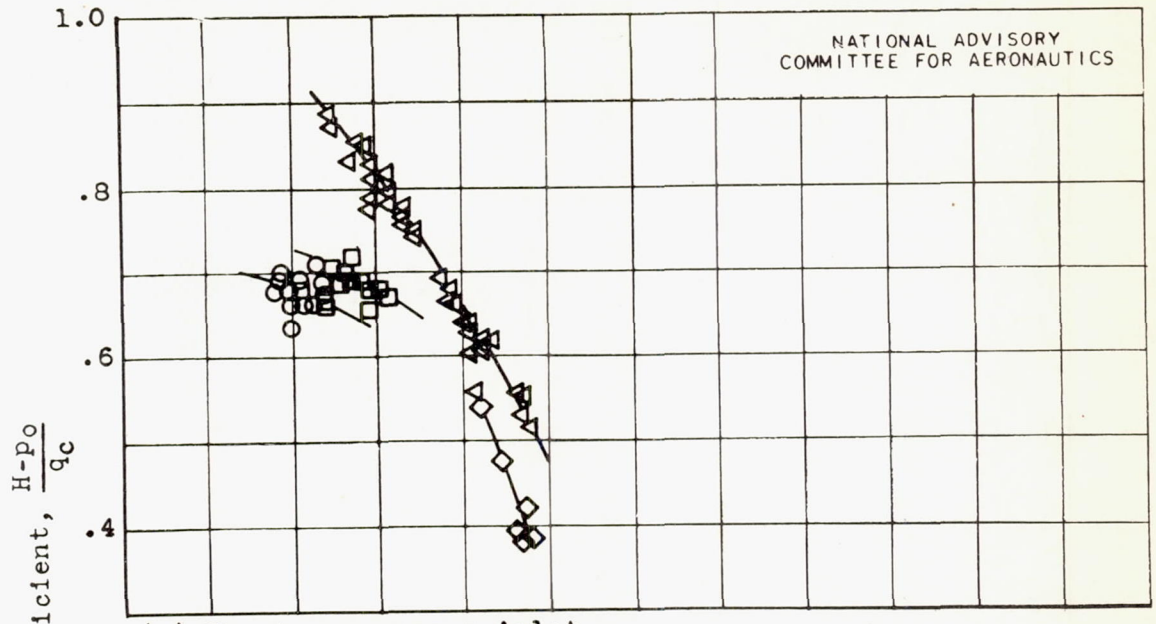

(a) Front compressor inlet.

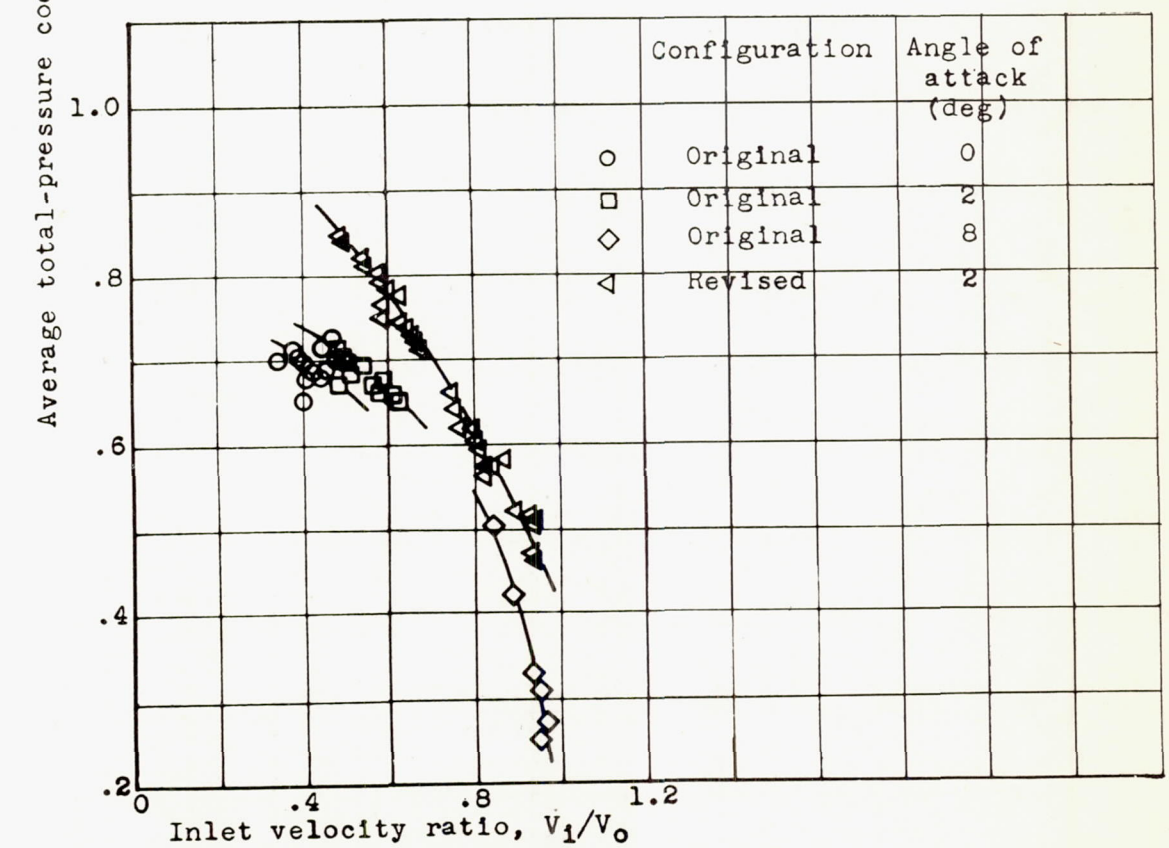

(b) Rear compressor inlet.

Figure 14.- Variation of average total-pressure coefficient at inlets of compressor with nacelle-inlet velocity ratio of fighter airplane.

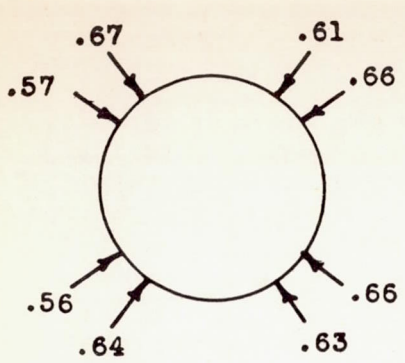

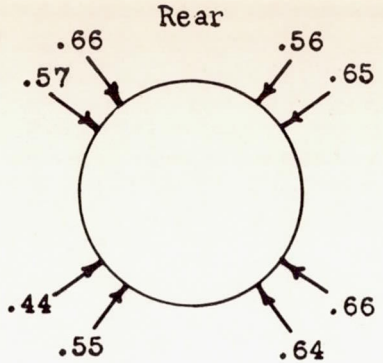

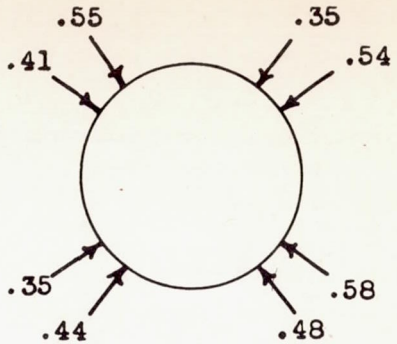

NATIONAL ADVISORY
COMMITTEE FOR AERONAUTICS

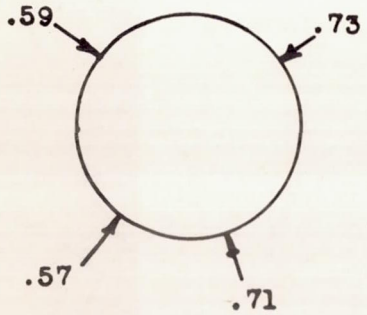

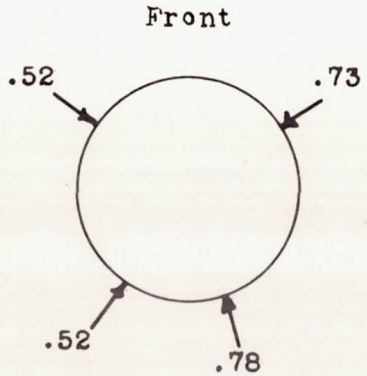

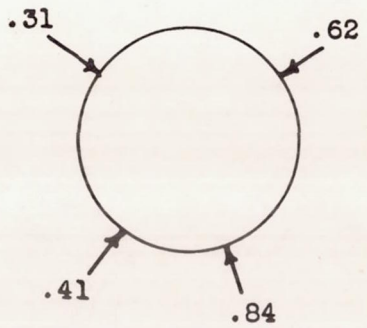

(a) Inlet velocity ratio, 0.47; Mach number, 0.46; Reynolds number, 8.6×10^6.

(b) Inlet velocity ratio, 0.54; Mach number, 0.42; Reynolds number, 13.7×10^6.

(c) Inlet velocity ratio, 0.74; Mach number, 0.27; Reynolds number, 14.5×10^6.

Figure 15.- Total-pressure coefficient of air entering front and rear inlets of left engine compressor. Fighter airplane; original configuration; angle of attack, 2°.

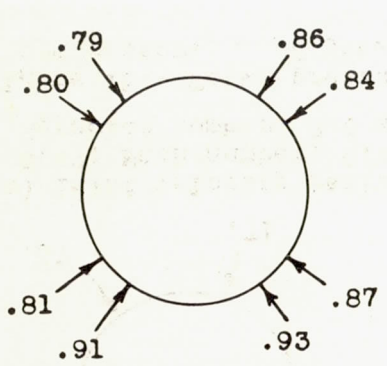

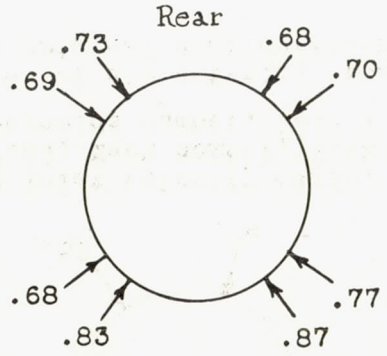

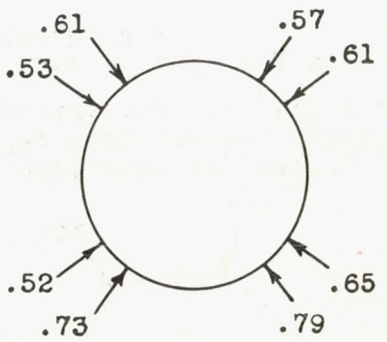

NATIONAL ADVISORY
COMMITTEE FOR AERONAUTICS

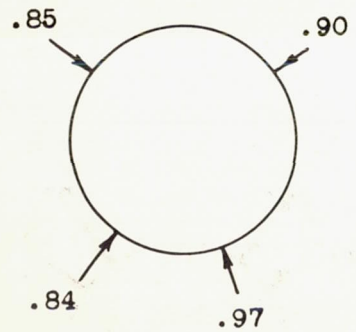

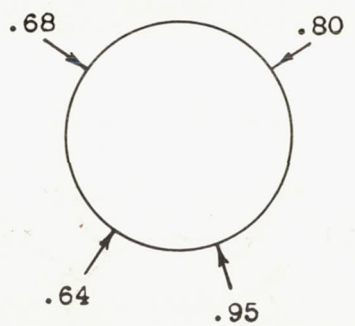

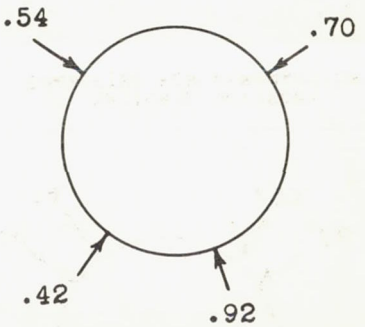

(a) Inlet velocity ratio, 0.50; Mach number, 0.49; Reynolds number, 9.5×10^6.

(b) Inlet velocity ratio, 0.65; Mach number, 0.42; Reynolds number, 15.3×10^6.

(c) Inlet velocity ratio, 0.80; Mach number, 0.30; Reynolds number, 6.1×10^6

Figure 16.- Total-pressure coefficient of air entering front and rear inlets of left engine compressor. Fighter airplane; revised configuration; angle of attack, 2°.

NACA MR No. E5L17

E-274

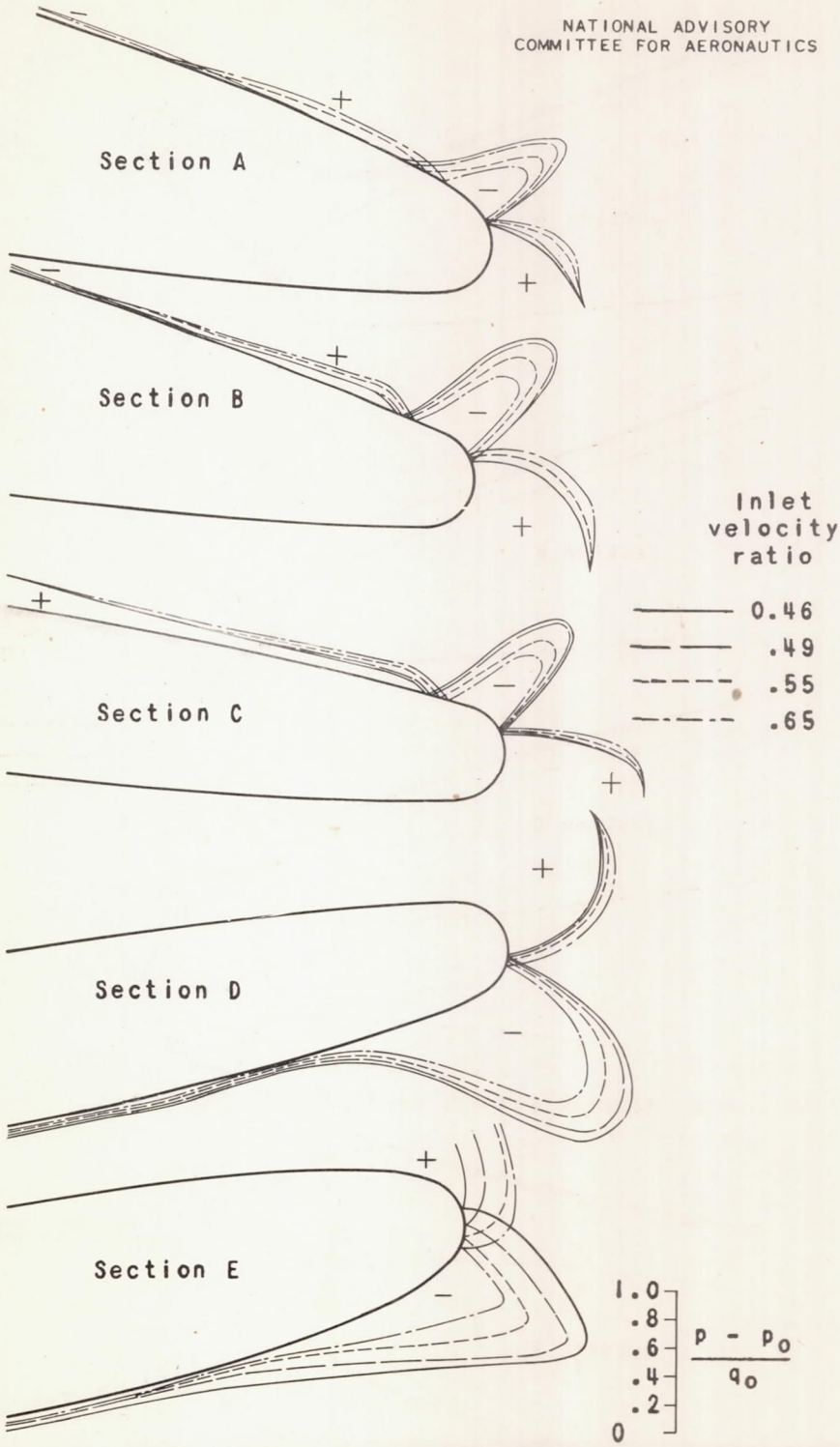

(a) Original nacelle inlet; angle of attack, 0°.

Figure 17. - Surface pressure distributions at nacelle-inlet lips of fighter airplane. Free-stream Mach number, 0.25; length of section shown, 9 percent of nacelle length.

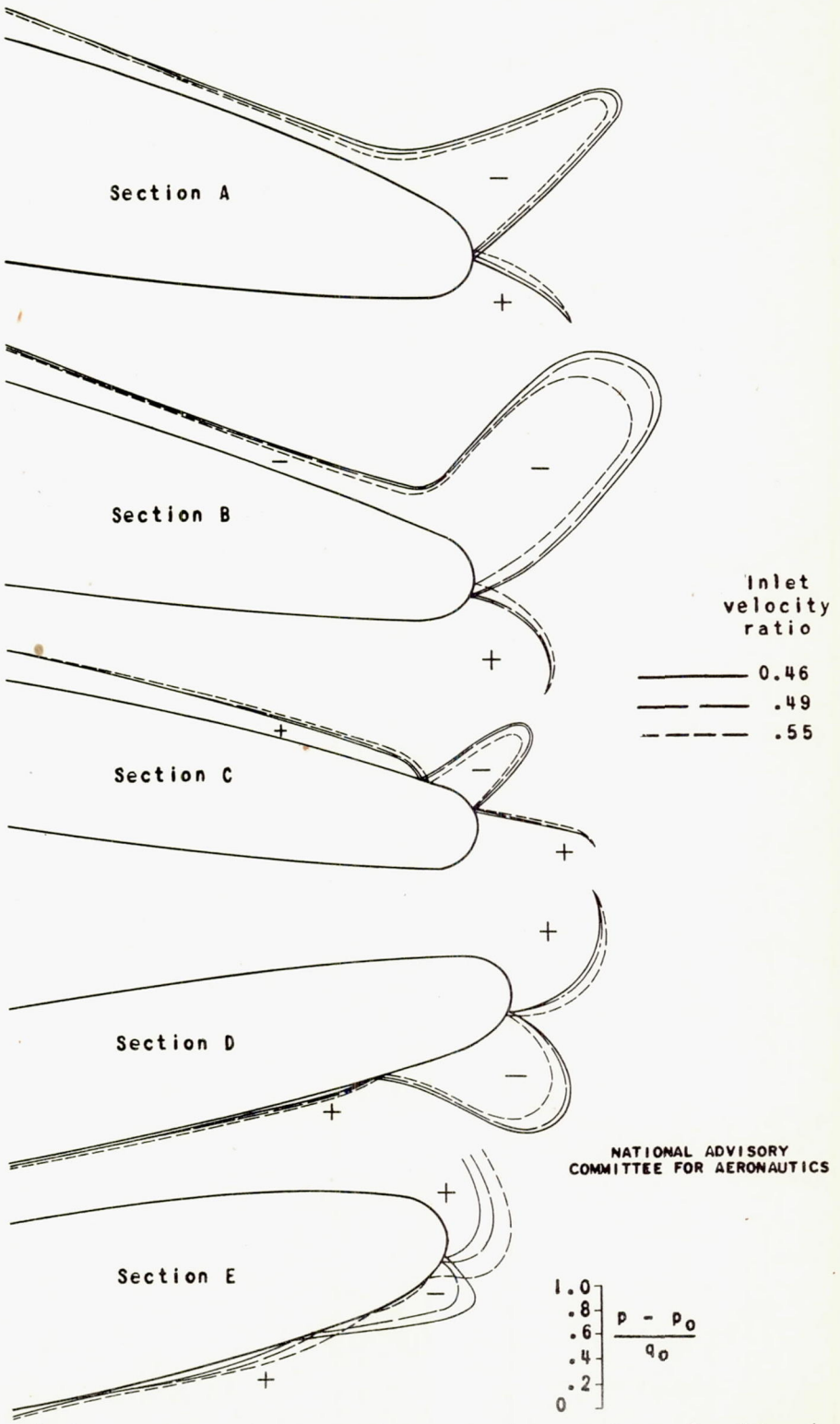

(b) Original nacelle inlet; angle of attack, 2°.

Figure 17. - Continued.

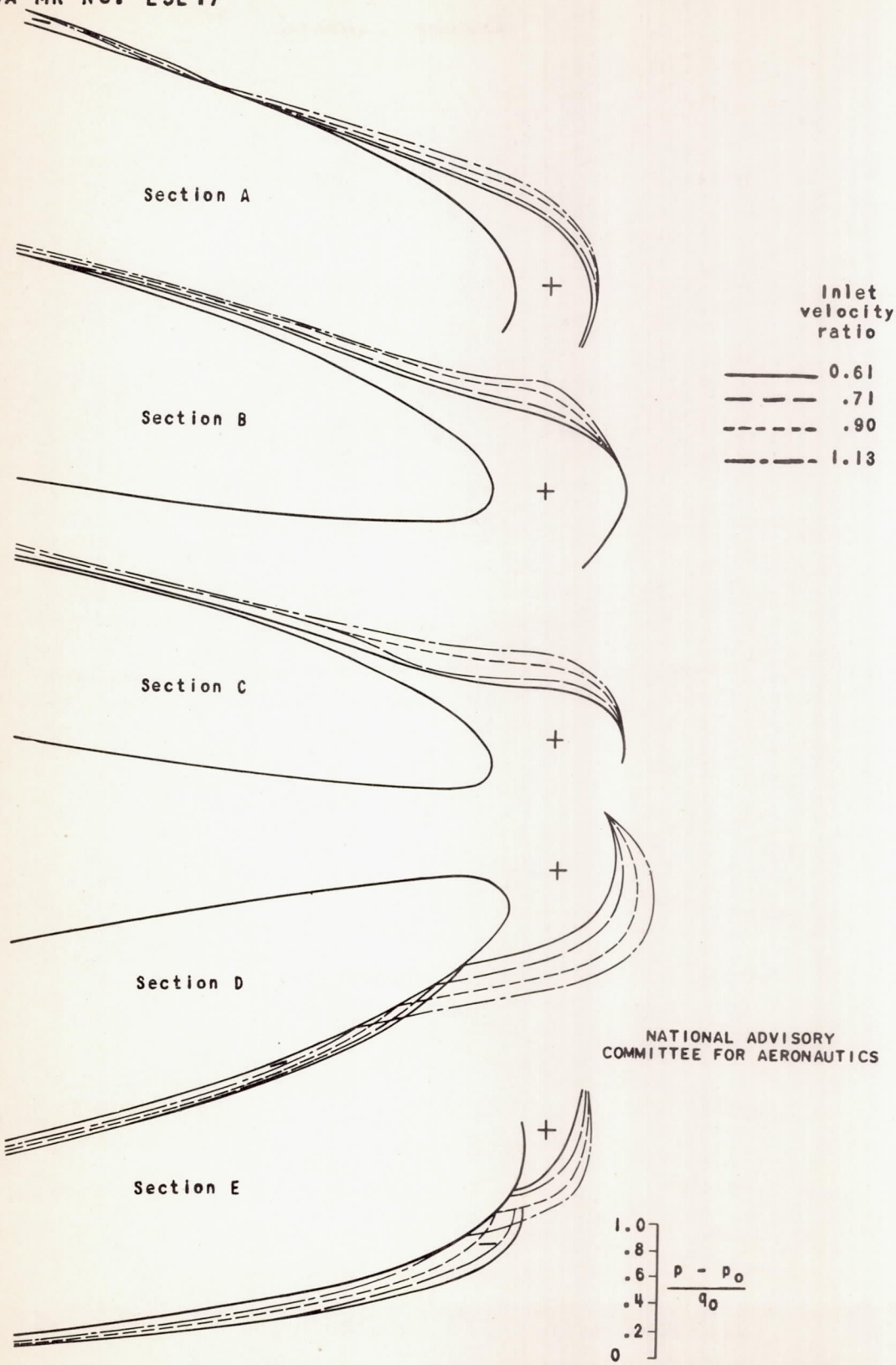

(c) Revised nacelle inlet; angle of attack, 0°.

Figure 17. - Continued.

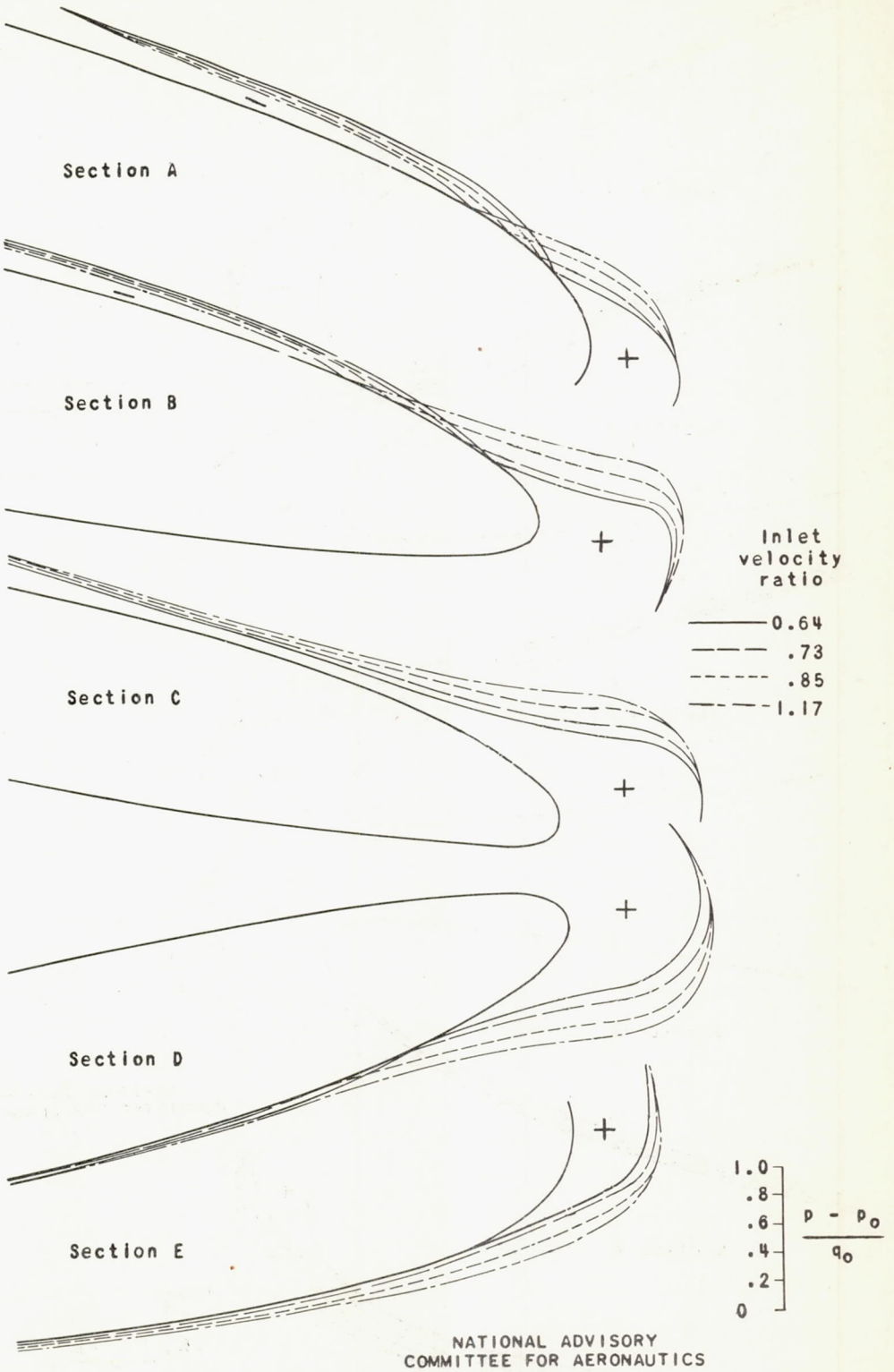

(d) Revised nacelle inlet; angle of attack, 2°.

Figure 17. - Concluded.

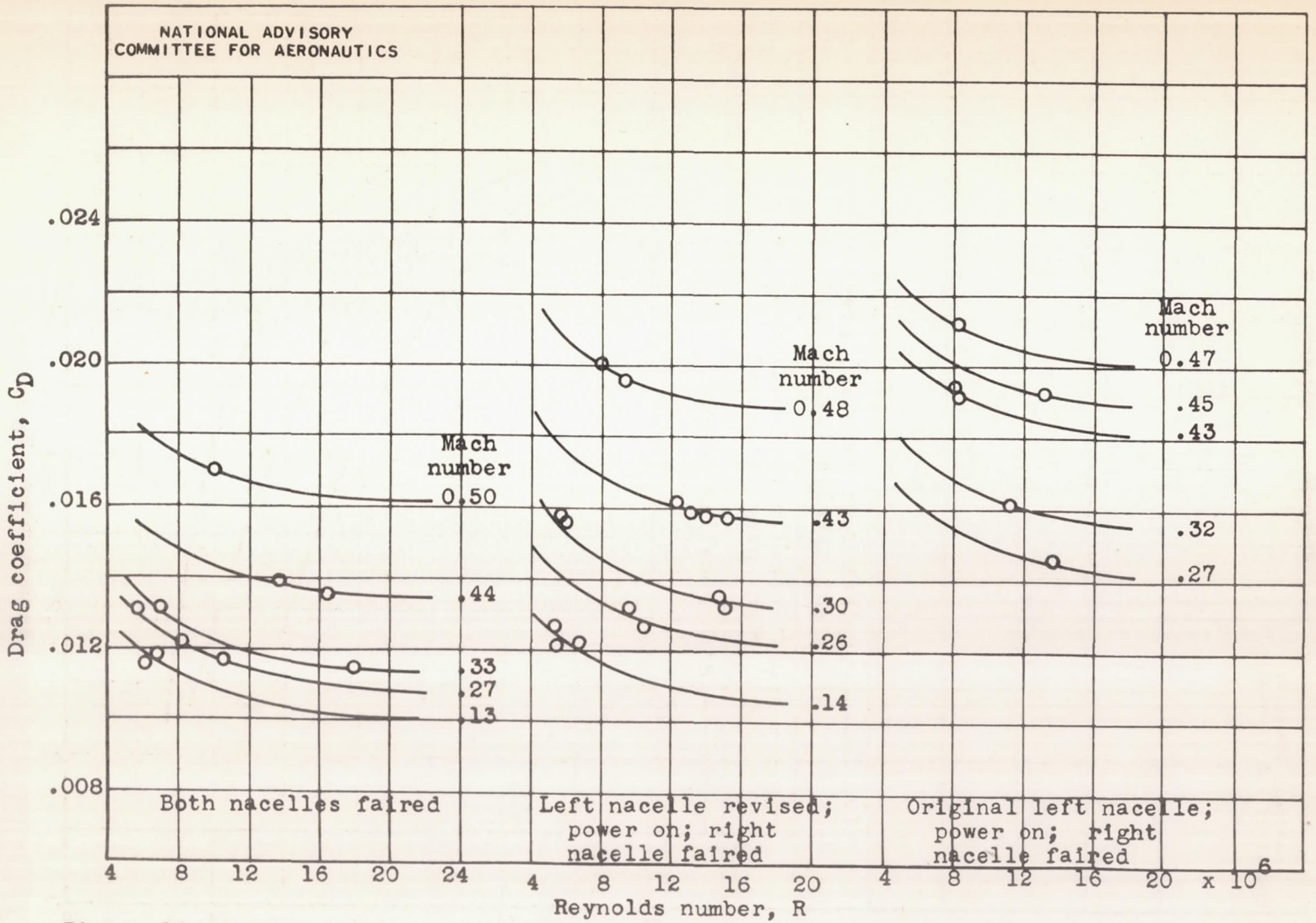

Figure 18.- Variation of drag coefficient with Reynolds number for various free-stream Mach numbers and test configurations of fighter airplane. Engine speed, 16,410 rpm.

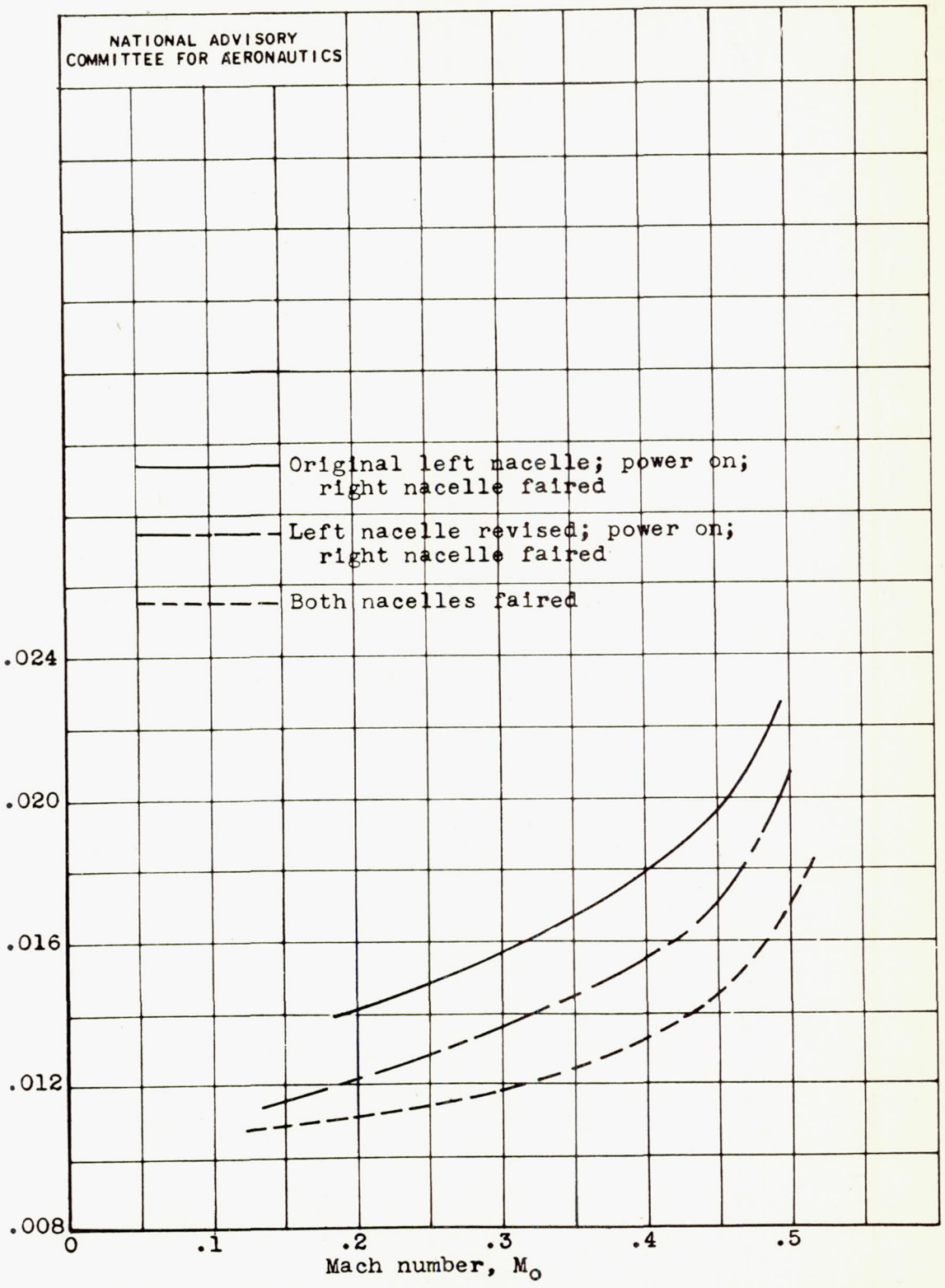

Figure 19.- Variation of drag coefficient with free-stream Mach number for various configurations of fighter airplane. Reynolds number, 10×10^6; engine speed, 16,410 rpm.